EPJ manuscript No.
(will be inserted by the editor)

submitted to Eur. Phys. J. AP

Tuning growth from clusters to continuous ultrathin films : Experiments and molecular dynamics simulations of Pd plasma sputter deposition.

Pascal Brault[1,a], Anne-Lise Thomann[1], Caroline Andreazza-Vignolle[2], and Pascal Andreazza[2]

[1] Groupe de Recherches sur l'Energétique des Milieux Ionisés, UMR6606 CNRS-Université d'Orléans BP 6744, 45067 Orléans Cedex 2, France
[2] Centre de Recherche sur la Matière Divisée, UMR6619 CNRS-Université d'Orléans, 45071 Orléans Cedex 2, France.

Received: December 18, 2001 / Revised version: June 12, 2002

Abstract. Plasma sputter deposition experiments and simple molecular dynamics calculations are performed for highlighting the effects of plasma ions and kinetic energy of palladium atoms on the morphology of thin films. A transition between cluster and continuous film growth is observed. It is attributed to the kinetic energy of the depositing sputtered palladium atoms and to high binding energy trapping sites resulting from the effects of ions incident on the surface during deposition. These high binding energy trapping sites act as additional nucleation centres that are allowed to be visited by the diffusing Pd atoms.

PACS. 81.15.Cd Deposition by sputtering – 68.55.Av Nucleation and growth - Microscopic aspects – 31.15.Qg Molecular dynamics and other numerical methods

1 Introduction

Growth of transition metal thin films on amorphous substrates is of great interest in various applications such as catalysis. In this case, it is often required that growth occurs through clusters [1,2]. On the other hand, it is also interesting to obtain continuous thin film of low thickness, as for hydrogen purification [3]. Up to now it seems difficult to obtain continuity at very low thickness (< 100 Å) with transition metals due to their strong cohesive energy [4]. Continuous thin films are rather reached for thicknesses above 1000 Å. Experiments on sputter plasma deposition show that growth occurs through particular modes due to the simultaneous exposition of a substrate to metal atoms (Pd) and plasma ions (Ar^+) at room temperature on a-C and a-SiO_2 substrates [5–8]. A transition between cluster growth and continuous thin film is obtained when increasing kinetic energy E_{Pd} of Pd atoms and with a ratio of ion flux to metal atoms flux $\frac{\phi_{Ar^+}}{\phi_{Pd}}$ in the range 3-8. For investigating the role of the metal atom kinetic energy on the growth morphology, Molecular Dynamics (MD) calculations are conducted within the frame of the stochastic classical trajectory ghost atom theory [9,10]. Our main goal is to provide a simple way for simulating growth processes describing experiments [5–8]. The effects of ions are modelled by artificially increasing the binding energy of the condensing atoms on the surface. Indeed, the one of the well known effect of plasmas is to increase sticking by creating point defects [11]. Some other effects can take place such as energy transfer from incident ions to adsorbate. Cluster shape can be also affected by ion collisions.

In the next section, experimental results of plasma sputter deposition of Pd onto amorphous carbon are described. The third section is devoted to MD simulations. Finally, a conclusion summarises the work.

2 Experiments

The experimental setup dedicated to the study of metal cluster growth using plasma sputter deposition has been widely described elsewhere [5–8]. A low pressure (1-100 mTorr) high frequency (100 MHz) plasma is created in argon gas with input power of several Watts. The palladium atom source (helicoidal wire) is negatively biased (V_b = -350 V) so that the ions gain sufficient energy to induce sputtering. Then sputtered Pd atoms can reach the substrate and growth starts. The substrate is chosen to be an amorphous carbon membrane coated on a copper grid for allowing direct Transmission Electron Microscopy (TEM)

[a] e-mail: Pascal.Brault@univ-orleans.fr

Table 1. Deposition parameters : P is the argon working pressure. At the substrate, $E_{Ar+}^{substrate}$ is fixed around 50 eV. ϕ_{Pd} is the Pd deposition rate and ϕ_{Ar+} is the ion flux at the surface. E_{Pd} is the depositing Pd atom kinetic energy.

P (mTorr)	ϕ_{Ar+} ($cm^{-2}s^{-1}$)	ϕ_{Pd} ($cm^{-2}s^{-1}$)	ϕ_{Ar+}/ϕ_{Pd} (-)	E_{Pd} (eV)
100	2.0 10^{14}	6.3 10^{13}	3	0.026
1	8.0 10^{14}	1.0 10^{14}	8	1.20

analysis. A very important feature is that the substrate is continuously bombarded by Ar^+ ions during the deposition. The corresponding ion kinetic energy $E_{Ar+}^{substrate}$ remains constant. It is evaluated to about 50 eV. Main parameters of the deposition process have been identified to be the ion flux ϕ_{Ar+}, the Pd atom flux ϕ_{Pd}, and the Pd atom kinetic energy E_{Pd} [7,8]. Deposition rates were measured by Rutherford Backscattering Spectrometry using a 2 MeV α particle beam extracted from a Van de Graaf accelerator. E_{Pd} is simply tuned by varying the pressure. This value corresponds to the maximum of energy distribution function of sputtered atoms. Indeed, sputtered atom kinetic energy is given by the Thompson formula [12,13]. Essentially, in vacuum ion sputtering, the energy E_{Pd} of the maximum of the distribution is given by half the cohesive energy E_{coh} (for Pd E_{coh}=3.89 eV) and the width of the distribution is rather large. When a buffer gas is present, as in plasma sputtering, E_{Pd} is shifted to lower energy depending on the gas pressure [13] and the distribution width is narrowed. The minimum reachable value corresponds to the gas temperature and the distribution becomes Maxwellian. In the present study, E_{Pd} = 1.2 eV and 0.026 eV (complete thermalization), which corresponds to sputter gas pressure of 1 and 100 mTorr respectively. Thus in plasma sputtering the kinetic energy can be varied from gas temperature to $\frac{1}{2}E_{coh}$. This situation is quite different than in classical evaporation where the directed kinetic energy is around 0.1 eV. The plasma conditions investigated here are summarized in Table 1.

Fig. 1 displays a set of micrographs for the two conditions of Table 1. Figs. 1(a-c) correspond to P= 100 mTorr, V_b=-350 V.In that case [7], it was shown that growth kinetics obey the power law <d> $\propto t^{\alpha}$; with α = 0.25 and <d> being the elementary cluster diameter. It was demonstrated that incident ions during growth were responsible for atom surface diffusion leading to the cluster growth. Fig. 1(d-f) display TEM micrographs when the ratio $\frac{\phi_{Ar+}}{\phi_{Pd}}$ is slightly increased (from 3 to 8) and Pd kinetic energy is considerably larger, E_{Pd} = 1.2 eV. This is obtained by lowering argon pressure to 1 mTorr (see Table 1). One can observe, at n_{Pd} = 8.0 10^{15}at.cm^{-2} (Fig. 1), that percolation is rapidly reached and that growth is more two-dimensional contrary to the preceeding case. Thus, when increasing deposition time, for this condition, a fully continuous layer is obtained with a thickness of 80 Å (Fig. 1f). This is very unusual because, in classical evaporation, a continuous layer is obtained for thicknesses larger than 1000 Å. For better understanding, it is interesting to compare both evolutions. In Figs. 1a and 1d cluster densities are respectively 3.5 10^{12} cm^{-2} and 5.6 10^{12} cm^{-2} while the mean cluster radius <d> is the same for both cases i. e. <d> = 3 nm. One could attribute such a difference in cluster densities to the excess of incident ions at low coverage that create trapping sites. Simultaneously, the greater kinetic energy allows to visit these sites and incoming atoms can be trapped when sufficient kinetic energy is lost to the substrate. Another possibility is that ions can "cut" the clusters which also leads to a higher density. But at low coverage this is less probable than creating defects on large open aeras. The role of trapping site will be addressed in the simulation section. When increasing Pd loading to around 10. 10^{15}at.cm^{-2} Figs. 1b and 1e display completely different morphology of Pd deposits after cluster coalescence is started. On Fig 1b, clus-

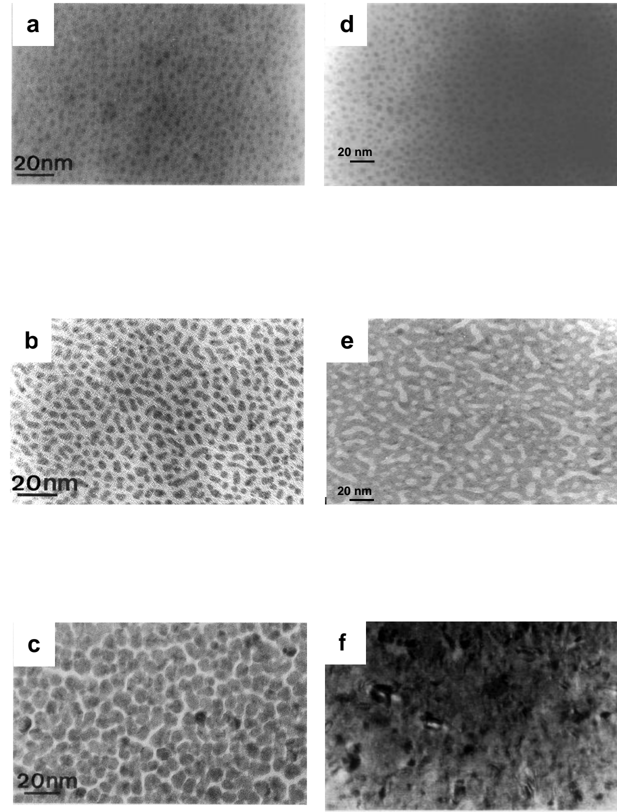

Fig. 1. Pd growth for the two plasma conditions illustrated by (a-c) TEM micrographs at P=100 mTorr and by (d-f) TEM micrographs at P=1 mTorr (see Table 1) where Pd loading n_{Pd} is increased. (a) n_{Pd}=3.8 10^{15}at.cm^{-2} and <d> = 3.0 nm (b) n_{Pd}=8.0 10^{15}at.cm^{-2} and <d> = 3.5 nm (c) n_{Pd}=60. 10^{15}at.cm^{-2} and <d> = 6.0 nm (d) n_{Pd}=3.0 10^{15}at.cm^{-2} and <d> = 3.0 nm (e) n_{Pd}=12. 10^{15}at.cm^{-2} and <d> is no longer defined and percolation is already reached. (f) n_{Pd}=60. 10^{15}cm^{-2} and a dense continuous layer is growing. Dark zones are Pd covered areas.

ter are always present and for Fig 1e, the growth is more two-dimensional and clusters have disappeared resulting is a percolated structure where now voids (white areas in Fig. 1e) are isolated instead of Pd clusters. Departure from cluster growth comes from a combined effect of ions and depositing atom kinetic energy. Indeed, when increasing their kinetic energy, Pd atoms can travel a longer time without interacting with existing cluster or trapping sites, contrary to slower atoms, which are more readily trapped either by a close existing cluster or by an efficient trapping site. Moreover increasing ion to depositing atom flux ratio results in more numerous trapping sites and also allows surface cluster atoms to move more easily especially at the border of the cluster which flattens it. Indeed, ion impacted surface atoms have now enough energy for leaving the top of the cluster and to become trapped at the border or far from the cluster. This is a necessary way , if we expect this effect to be efficient in causing continuous layer growth. In those cases, the growth conditions become favourable to prevent 3D cluster growth to the benefit of lateral growth leading to continuous layer of very low thickness (see Fig 1e, f)

3 Molecular dynamics simulations

For clarifying the mechanisms involved in the growth transition from clusters to continuous film, we performed Molecular Dynamics simulations. Ghost atom theory is used for simplifying the calculations. Thus, assuming pairwise additive interactions, the motion of mobile atoms are given by the Newton set of equations:

$$m_j \frac{\partial^2}{\partial t^2} x_j = -\frac{\partial}{\partial x_j} V_s - \sum_{i \neq j} \frac{\partial}{\partial x_j} V_{ij} \quad (1)$$

$$m_j \frac{\partial^2}{\partial t^2} y_j = -\frac{\partial}{\partial y_j} V_s - \sum_{i \neq j} \frac{\partial}{\partial y_j} V_{ij} \quad (2)$$

$$m_j \frac{\partial^2}{\partial t^2} z_j = -\frac{\partial}{\partial z_j} V_s - \sum_{i \neq j} \frac{\partial}{\partial z_j} V_{ij} \quad (3)$$

where the mobile atoms have positions x_j, y_j (lateral positions), z_j (height above the surface), j=1,..., N atoms, with masses m$_j$. $V_s = V_s(x_j, y_j, z_j, s_j)$ is the interaction potential between atom j and the surface. $V_{ij} = V_{ij}(x_j, y_j, z_j, x_i, y_i, z_i)$ is the pair interaction potential between atoms j and i. The s_j is the coordinates of the ghost atom (i.e. the magnitude of the perturbed oscillations of the ghost) associated to the jth incident atom (i.e. the normal projection along the z-axis). It obeys the Langevin-type equations of motion along the z-axis:

$$m_s \frac{\partial^2}{\partial t^2} s_j = -\frac{\partial}{\partial s_j} V_s - K s_j - m_s \beta \frac{\partial}{\partial t} s_j + R_j \quad (4)$$

where m_s is the surface real atom mass. Taking account of the motion only along the z-coordinates is justified by the fact that energy exchanges are essentially perpendicular to the surface [10]. The friction constant β and the force constant K are chosen for representing the real surface [10]:

$$\beta = \frac{\pi \omega_D}{6} \text{ and } K = \frac{m_s \omega_s^2}{3}$$

where $\omega_s (= \frac{2}{3}\omega_D$ [14]), is the surface Debye frequency normal to the surface ($\hbar\omega_D = k_B T_D$, T_D is the Debye temperature, T_D=2230 K for C). The R_j are gaussian random forces with a "white spectrum". The strength A of this force is related to the friction constant β and the surface temperature T_s through the fluctuation-dissipation theorem: $A = 2\beta m_s k_B T_s$. Thus the R_j appearing in equation (4) are randomly selected from a gaussian distribution with a width $\sigma = \left[\frac{2\beta m_s k_B T_s}{dt}\right]^{\frac{1}{2}}$, where dt is the integration time step [10,11]. This allows the averaged temperature of the surface T_s to be maintained by choosing A. T_s is fixed to 300 K. For integrating the equation of motion we used the velocity form of the Verlet algorithm [15], which allows a good definition of the velocities. Velocities are required for integrating the stochastic equation (4). This algorithm is time reversible, and has a long time stability [16]. Pd deposition was conducted on a model amorphous carbon surface. For Pd-Pd interactions, we use a Lennard-Jones potential with the parameters found in the literature [17]: $V_{Pd-Pd} = 4\epsilon_{Pd}\left[\left(\frac{\sigma_{Pd}}{r}\right)^{12} - \left(\frac{\sigma_{Pd}}{r}\right)^{6}\right]$, with $\epsilon_{Pd} = 0.426$ eV and $\sigma_{Pd} = 2.52$Å. The Pd-C Lennard-Jones interaction potential is obtained by using the Lorentz-Berthelot mixing rule [18]: $\epsilon_{Pd-C} = (\epsilon_{Pd}\epsilon_C)^{\frac{1}{2}}$ and $\sigma_{Pd-C} = \frac{(\sigma_{Pd}+\sigma_C)}{2}$. The parameters for C-C interactions can be found in reference [19] and the values are: $\epsilon_C = 2.414\ 10^{-3}$ eV and $\sigma_C = 3.40$ Å. This gives: $\epsilon_{Pd-C} = 0.0327$ eV and σ_{Pd-C} = 2.99 . In the present work, no surface atomic corrugation (contrary to Refs. [10,11]) is introduced, which means that no preferential adsorption sites are expected on amorphous carbon. The Pd atoms were randomly placed at a cut-off distance z_c=2.5σ_{Pd-C} above the surface and were launched each after each other. The time step is fixed to dt=1 fs. The delay between two atom injections is 500 fs. This is sufficient to avoid interactions in the gas phase. One could guess that this involves an unphysically large flux, but it was observed that increasing this delay does not change the results. This is due to the way that energy is released in the pseudo-bulk by ghost atoms. Such a delay was also used for deposition of Pt on graphite [18] and in many other works : using realistic values will render such molecular dynamics calculations impossible. The velocities are randomly chosen in a Maxwell distribution. A velocity component directed towards the surface is added for simulating high velocity of sputtered atoms in a low pressure ambient gas. All the atoms interact among themselves at any times within their cut-off radius, 2.5σ_{Pd-C}. This is necessary for allowing the clusters to move freely. Because equation (4) only allows surface temperature accomodation of the atoms that directly bind to the surface, it is necessary to reset the velocities of cluster atoms. Simply, if an atom is sufficiently bound to other atoms (

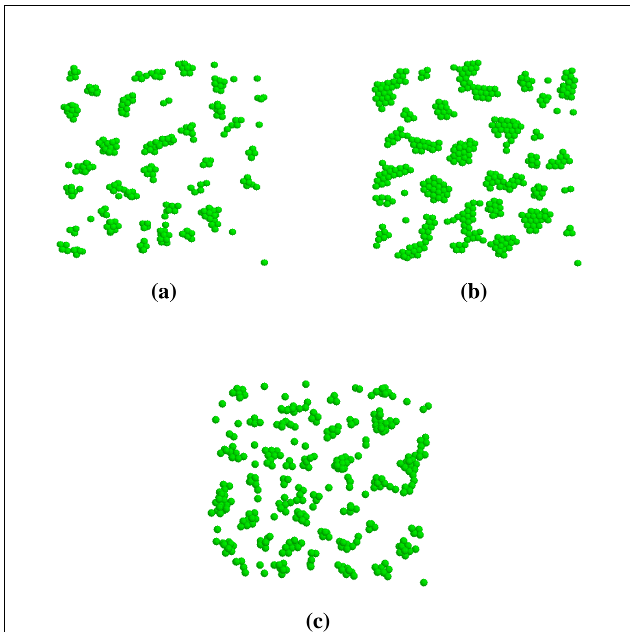

Fig. 2. Snapshot of the palladium clusters at 0.3 ML deposition on a 100x100 $\AA^2$ a-C surface. (a) ϵ_{Pd-C} = 0.0327, E_{Pd} = 0.026 eV and S=0.6, (b) ϵ_{Pd-C} = 0.327, E_{Pd} = 0.026 eV and S=0.9, (c) ϵ_{Pd-C} = 0.327, E_{Pd} = 1. eV and S=0.75 (a filled ball stands for a single atom)

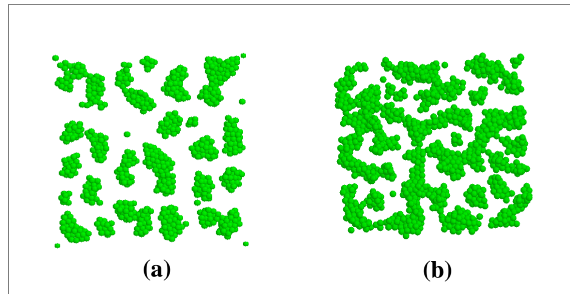

Fig. 3. Snapshot of the palladium clusters at 1 ML deposition on a 100x100 Å a-C surface showing the transition from cluster to continuous growth. (a) ϵ_{Pd-C} = 0.1 eV, E_{Pd} = 0.026 eV and S=0.6, (b) ϵ_{Pd-C} = 0.327, E_{Pd} = 1.0 eV and S=0.75)

$\sum_{i\neq j} V_{ij}$ < -0.3 eV [20]), its velocity is reset to a random velocity in a Maxwell distribution at T_s. The size of the surface is 100x100 $\AA^2$. One monolayer (ML) corresponds to 1521 atoms as defined for an ideal Pd monolayer in the fcc(111) surface structure. The calculations have been performed at 0.3 ML (457 Pd atoms) and 1 ML for two values of ϵ_{Pd-C} : 0.0327 (the expected value) and 0.327 eV. This latter value, which models the ion effects in rendering nucleation sites more binding, is consistent with experimental ones [21]. After deposition of all atoms, a subsequent run including all the adsorbed atoms is performed for allowing complete relaxation after deposition. This is mainly needed for the last launched atoms. This equilibration phase lasts 10 ps. A run with 457 atoms takes 239 ps and with 1521 atoms takes 770 ps. Note that escaping atoms due to desorption are free to go back in the gas phase. This allows calculating the sticking coefficient S at each time step. In Fig. 2, are plotted the films at 0.3 ML. In Fig.2(a), ϵ_{Pd-C} = 0.0327 and E_{Pd}= 0.026 eV. The growth occurs through 3D clusters and S=0.6. This low S value is consistent with experimental published ones [2]. On figure 2(b), ϵ_{Pd-C} = 0.327 eV which stands for a more trapping site. This is also revealed by the high S value: S = 0.9. In this case, the aggregates are two-dimensional. This comes from the high trapping energy, which competes with the Pd-Pd interaction. Due to the low kinetic energy they are not able to form 3D clusters, because the atoms are impeded to climb on the cluster and the interaction energies between atoms are not sufficient for reorganisation as 3D clusters. When ϵ_{Pd-C} = 0.327 and E_{Pd} = 1. eV (figure 2(c)), the 3D cluster growth is recovered, because of the higher initial kinetic energy allowing the atoms to climb on an existing cluster. But when comparing to 3D-cluster growth in figure 2(a), the cluster density is increased and isolated atoms are more numerous, because S=0.75. In fact the high energy trapping sites play always a role even for high kinetic energy. Even if the atoms can diffuse a longer time and visit more sites due to their kinetic energy, they also loose energy along diffusion due to the interaction with the surface (equation 4). Thus they find a binding site, but now with equivalent probabilities for remaining isolated and trapped or for sticking to an existing cluster. The sticking coefficient, S=0.75, is lowered, compared to Fig. 2, by the increased reflection probability: atoms with sufficient kinetic energy may more easily feel the repulsive part of the Pd-C or Pd-Pd potentials, which results in desorption. In Fig. 3, is plotted a later stage of growth i.e. after launching 1521 Pd atoms. This is performed for ϵ_{Pd-C} = 0.10 and E_{Pd} = 0.026 eV (figure 3a), and ϵ_{Pd-C} = 0.327 eV and E_{Pd} = 1.0 eV (figure 3b). ϵ_{Pd-C}= 0.0327 was no more used, because large desorption inherent to the use of Lennard-Jones potential was effective at higher coverages [22]. Low interaction with the surface at low kinetic energy results in 3D-cluster growth with a low level of meandering. Moreover S=0.6, indicating desorption remains effective but in a reasonable range compared to experiments [2]. At high interaction with the surface and high kinetic energy, the percolation of 3D clusters is already reached (figure 3b). This is consistent with the situation at low coverage (figure 2c) where isolated trapped atoms play the role of additional nucleation sites. Thus meandering islands get quickly in contact, ensuring quick percolation. Moreover, the sticking coefficient S=0.75 (figure 3b) is greater than in the former situation (figure 3a), which makes more atoms available for allowing quick percolation. This stage is in fact precursor to a quickly growing continuous film. This becomes possi-

ble because the adsorbate initial kinetic energy allows site visiting more complete and trapping energy reduces desorption. Such behaviour is thus in perfect agreement with the experiments reported in section 2 (Figs. 2b and f). One can also expect that increasing further kinetic energy, will slow down the rapid percolation, in the way similar to the transition between 2D and 3D cluster growth (Fig. 2b, c). It is interesting to note that, in all the conditions examined here, clusters were observed to move except in the 2D growth (figure 2b)) where the clusters are too much bound to the substrate. Thus a convenient choice between trapping energy and adsorbate initial kinetic energy allows a transition from cluster to continuous film growth, which is of particular interest for transition metals [3].

4 Conclusion

Plasma sputter experiments and a simple model based on molecular dynamics calculations were carried out for examining 2D, 3D and continuous thin film growth. The role of trapping site energy resulting from plasma ion effects at the surface and initial kinetic of the adsorbates are clearly evidenced to be the main parameters for controlling the growth modes of Pd onto amorphous carbon. Especially at coalescence, the growth can be oriented towards cluster or continuous film growth.

References

1. C. T. Campbell, Surf. Sci. Rep. 27, 1 (1997)
2. C.R. Henry, Surf. Sci. Rep 31, 231 (1998)
3. J. N. Armor, Catalysis Today 25, 199 (1995); J. Shu, B. P. A., A. Van Neste, S.Kaliaguine, Can. J. Chem. Eng. 69, 1036 (1991)
4. Venables J A, Spiller G D T and Handbücken M 1984 *Rep. Prog. Phys.* **47** 399
5. A.L. Thomann, P. Brault, C. Laure, B. Rousseau, H. Estrade-Szwarckopf, C. Andreazza- Vignolle, P. Andreazza, A. Naudon, Surface and Coatings Technology 98, 1228 (1998).
6. A.L. Thomann, P. Brault, J.P. Rozenbaum, C. Andreazza-Vignolle, P. Andreazza, H. Estrade-Szwarckopf, B. Rousseau, D. Babonneau, G. Blondiaux, J. Phys. D: Appl. Phys. 30, 3197 (1997).
7. P. Brault, A.L. Thomann, C. Andreazza-Vignolle, Surf. Sci. Lett. 406, L597 (1998)
8. A. L. Thomann, J. P. Rozenbaum, P. Brault, C. Andreazza-Vignolle, P.Andreazza, Appl. Surf. Sci. 158 (2000) 172 - 183
9. J. C. Tully, G. H. Gilmer, M. Shugard, J. Chem. Phys. 71, 1630 (1979)
10. P. Brault, J. de Almeida, Surf. Sci. 360, 43 (1996)
11. D. L. Smith, Thin-Film Deposition (Mc Graw-Hill, New York, 1995)
12. M. W Thompson, Philos. Mag 18, 377 (1968)
13. K. Meyer, I. K. Shuller, C. M. Falco, J. Appl. Phys. 52 5803, (1981)
14. B. J. Garrison and S. A. Adelman, Surf. Sci. 66, 253 (1977)
15. W. C. Swope, H. C. Andersen, P. H. Berens, K. R. Wilson, J. Chem. Phys. 76, 637(1982); M. P. Allen, D. J. Tildesley, Computer Simulations of Liquids; (Clarendon Press, Oxford 1987)
16. A. Omeltchenko, A. Nakano, K. Tsuruta, R. K. Kalia, P. Vashishta, Adv. Semicond. Clusters, 4, 263 (1998)
17. T. Halicioglu and G. M. Pound, Phys. Stat Sol. (a), 30, 619 (1975)
18. S. Y. Liem, K. Y. Chan, R. F. Savinell, Molecular Simulation 13, 47 (1994); G.-W. Wu, K.-Y. Chan, Surf. Sci. 365 (1996) 38; W. D. Luedtke and U. Landmann, Phys. Rev. B40, 11733 (1989)
19. W. A. Steele, Surf. Sci. 36, 317 (1973)
20. This value is chosen to ensure that the diffusion is not stopped. Above this value, too much atoms are accomodated and there is no further change below this value. It is dependent on the incident atom and the surface.
21. K. R. Heim. S. T Coyle., G. G. Hembree, J. A. Venables, J. Appl. Phys. 80, 1161 (1996)
22. L. J. Lewis, P. Jensen, J.-L. Barrat, Phys. Rev. B 56 (1997) 224